

# Evaluation of prior information in microwave tomography experiments for brain stroke detection

1<sup>st</sup> Olympia Karadima

Department of Engineering  
King's College London  
London, United Kingdom  
olympia.karadima@kcl.ac.uk

2<sup>nd</sup> Pan Lu

Department of Engineering  
King's College London  
London, United Kingdom  
pan.lu@kcl.ac.uk

3<sup>rd</sup> Ioannis Sotiriou

Department of Engineering  
King's College London  
London, United Kingdom  
ioannis.sotiriou@kcl.ac.uk

4<sup>th</sup> Panagiotis Kosmas

Department of Engineering  
King's College London  
London, United Kingdom  
panagiotis.kosmas@kcl.ac.uk

**Abstract**—This work examines the impact of prior information (or “initial guess”) for calibrating a microwave tomography system for brain stroke detection and differentiation, using a multi-layered, anatomically complex head phantom. The imaging algorithm applies the distorted Born iterative method (DBIM) combined with the two-step iterative shrinkage thresholding (TwIST) method. The initial guess for the algorithm is based on two models with different available information: one filled with the dielectric properties of average brain tissue, and one with a more accurate representation of the true head phantom. Our initial results demonstrate that the addition of thin head tissue layers (such as CSF) in the forward model is not critical for the successful reconstruction of the target's dielectric properties. As expected, however, we achieve more accurate results with the multi-layer initial guess in challenging cases such as detecting an ischemic stroke-like target in the presence of a six-layers Zubal head phantom.

**Index Terms**—DBIM, TwIST, microwave tomography, calibration, prior information, brain stroke

## I. INTRODUCTION

Brain strokes can be caused by a ruptured (hemorrhagic stroke) or a blocked (ischemic stroke) vessel. The quick and successful diagnosis of the stroke type is crucial, as the wrong treatment can be fatal for the patient [1]. The challenges of existing imaging techniques have motivated the development of novel applications that aspire to be fast, safe, portable and cost-effective [2].

Microwave imaging (MWI) [3] could potentially address the above requirements, forming an auspicious way to detect and monitor brain stroke in the pre-hospital stage or in the post-acute phase. MWI relies on potentially significant differences in the dielectric properties of the stroke relative to normal brain tissues, as a result of changes in the water content [4]. In microwave tomography (MWT) [5], this dielectric contrast allows obtaining a dielectric map of the imaging domain, and consequently, results in quantitative images of the possible diseased area.

MWT solves an inverse electromagnetic (EM) scattering problem, which is non-linear and ill-posed. Prior information can be incorporated into a MWT algorithm's “initial guess” [6] to calibrate the MWT system and increase its robustness and accuracy. Specifically for brain imaging, the high dielectric contrast between the different head tissues

adds an additional challenge to the successful detection and differentiation of brain stroke [7]. Therefore, there is a need to explore what prior knowledge is required to achieve a successful differentiation of the two stroke types in realistic imaging scenarios. This paper investigates this issue by testing detection in an anatomically complex head phantom with an “initial guess” that uses only an approximate model requiring little prior information.

The rest of the paper is organized as follows: Section II presents the head model based on the so-called “Zubal” phantom [8], as well as the MWT imaging system simulated on CST. It also details the DBIM-TwIST algorithm and the properties of the initial guess used together with the forward solver to calculate the EM fields. Section III reviews the reconstruction results obtained by the algorithm, followed by a Conclusion section.

## II. METHODS

### A. Simulations Setup

The proposed system and model are simulated using CST Microwave Studio®. Fig. 1 shows the simulated prototype that is composed by a tank with a diameter of 300 mm and is filled with 90% glycerol-water mixture. The imaging system is presented in detail in [9]. We place a six-layer brain model with base on an axial slice of the original MRI-derived Zubal head phantom [8], which emulates our experimental system with the phantom inside the tank. Each layer has dielectric properties of the equivalent head tissues assigned from CST's library. The dispersive dielectric properties of the model as well as the matching medium's are shown in Table I.

We place a cylindrical target (diameter  $d=20.3\text{mm}$  and height  $h=100\text{mm}$ ) inside the white matter area (in the left side of the phantom), which mimics either the hemorrhagic or the ischemic stroke. We increase the complexity of the Zubal phantom by adding one layer at each time while allocating the dielectric properties of average brain to the rest of the tissues. Fig. 1 shows our final six-layer phantom which includes skin, fat, bone, cerebrospinal fluid (CSF), grey matter, white matter, and the stroke-like target.

The phantom is surrounded by 16 printed monopole antennas [9] arranged in two elliptical rings with major and minor axes equal to 205mm and 148mm, respectively. We conduct three simulations for each scenario to acquire the scattered field data: one without the target (NT), one with hemorrhagic (h-stroke) and one with ischemic (i-stroke) stroke,

respectively. Overall, we examine five scenarios of different complexity, resulting into a total of 15 CST simulations.

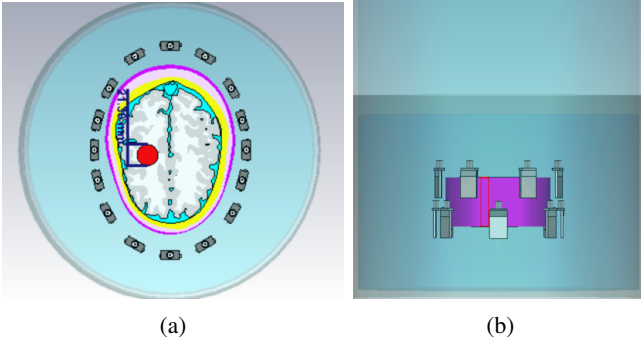


Fig. 1: The simulation system prototype in CST, which uses a numerical head model based on the Zubal head phantom. The head model's dimensions are approximately  $170 \times 130 \times 100 \text{ mm}^3$ .

### B. Distorted Born Iterative Method (DBIM) Method

The DBIM method solves the EM integral equation under the distorted Born approximation,

$$E_s(r_n, r_m) = E_t(r_n, r_m) - E_b(r_n, r_m) \\ = \omega^2 \mu_0 \epsilon_0 \int_V G_b(r_n, r) E_b(r, r_m) (O(r) dr) \quad (1)$$

where  $E_t$ ,  $E_s$  and  $E_b$  are the total, scattered and background fields respectively, while  $r_n$  and  $r_m$  demonstrate the transmitter and receiver positions and  $G_b$  represents the Green's function for the background medium. The contrast function  $O(r)$  denotes the difference between the complex permittivity of the reconstructed and the background permittivity. To calculate both  $E_b$  and  $G_b$ , we use the forward solver based on the finite-difference time-domain (FDTD) method [11].

While (1) is a two-dimensional TM integral equation, it can be used to implement the 3-D DBIM if we consider that cross-polarized electric fields are negligible [12], [13]. The ill-posed linear system resulting from discretizing (1) at each DBIM iteration is solved by the two-step iterative shrinkage thresholding (TwIST) method. The contrast function is calculated iteratively and is added to the background profile until the residual scattering is minimized.

To capture the frequency-dependence behaviour of the human tissues, we implement the single-pole Debye model for the complex permittivity:

$$\epsilon_s(\omega) = \epsilon_\infty + \frac{\Delta\epsilon}{1 + j\omega\tau} + j\frac{\sigma_s}{\omega\epsilon_0} \quad (2)$$

where  $\epsilon_\infty$ ,  $\Delta\epsilon$ ,  $\sigma_s$  and  $\tau$  are the Debye parameters. We assume that the relaxation time  $\tau$  is a known constant. The Debye parameters are calculated and updated iteratively until a convergence is reached [11]. This can be based on a fixed number of iterations or on minimising the difference between “measured” and calculated electric fields in (1).

### C. Imaging Methodology

We consider two “initial guess” scenarios that use different prior information of the phantom: the first considers a homogeneous ellipsoid filled with a dielectric that mimics the average brain tissue, while the second considers the exact multi-layer brain model used for the “measured data”. By

means of an example, Fig. 2 presents the models for the three and the six-layer Zubal phantom, as well as the model filled with only the average brain dielectric properties. Each layer of the forward model is assigned with the Debye parameters of the equivalent head tissue presented in Table I.

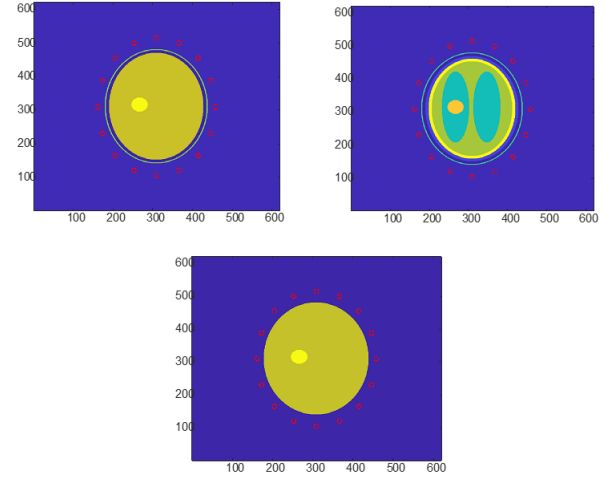


Fig. 2: Top views of the “initial guess” model for our three-layer (skin, fat, bone) head model (top left), our six-layer (skin, fat, bone, CSF, grey matter and white matter) head model (top right), and our homogeneous (average brain) head model (bottom). The outer layer's dimensions are  $170 \times 130 \times 100 \text{ mm}^3$ , as in Fig. 1.

TABLE I: Debye parameters of the forward model. The Debye parameters for the head tissues have been assigned by curve fitting from CST data. Debye parameters of the 90% glycerol-water and of the i-stroke have been obtained from experimental dielectric measurements which have been presented in [10].

Material type	$\Delta\epsilon$	$\epsilon_\infty$	$\sigma_s$
90% glycerol-water	6.56	16.86	0.3232
Average brain	45.8	0.1244	0.7595
Skin	41.17	11.15	0.6672
Fat	5.331	0.6564	0.037
Bone	11.59	1.932	0.0788
CSF	67.71	5.46	0.21
Grey matter	49.63	11.66	0.7
White matter	36.67	8.6	0.39
H-stroke	59.23	6.142	1.374
I-stroke	25	10	0.01

The algorithm models the antennas as point sources, which are placed at the same locations as the patch antenna's phase centers in the CST simulations. We use a “NT” reference scenario to calibrate the algorithm and account for sources of model's mismatch such as using approximate antenna models. The signal difference between the “with target” and the “no target” scenarios will depend on the initial guess model, leading to a different calibration for the three different models shown in Fig. 2.

To deal with computational complexity of the 3-D implementation, we followed the implementation in [13], which employs the Nvidia GPU Tesla K20c and implements the 3-D FDTD forward solver with CUDA to accelerate its run time. We then used Matlab MEX functions to integrate the GPU code with our DBIM code in Matlab. The implementation

is based on Matlab R2020b, CUDA 8.0 and VS 2015. The elapsed time for each antenna is 81 seconds, meaning that the running time for each iteration is roughly 22 minutes when using 16 monopole antennas.

To evaluate our reconstructions, we use a normalised reconstruction error based on the estimated  $\epsilon_\infty$  in the target area, which is defined as,

$$er = \frac{\|\epsilon_\infty^{original} - \epsilon_\infty^{reconstructed}\|^2}{\|\epsilon_\infty^{original}\|^2} \quad (3)$$

In all our reconstructions, we chose a fixed number of 20 iterations which balances the requirements for convergence and run time.

### III. RESULTS

Figs. 3-7 present the dielectric constant distribution at a horizontal cross-section, as reconstructed by the 3-D DBIM-TwIST at 1.0 GHz for the case of h- and i-stroke respectively. The size of the 3-D domain is  $100 \times 100 \times 100$  in resolution of 2 mm. The figures compare results from our two imaging scenarios, i.e., using a homogeneous vs. the exact head model (without the target) as prior information for calibration, for complex phantoms of increasing complexity based on adding tissue layers from the original head model in Fig. 1.

Figs. 3-6 show that we achieve similar reconstructed images for both stroke targets by using the homogeneous or the multi-layer head model as our calibration reference. Moreover, the reconstructed values of the stroke targets are closer to their real values when using the homogeneous forward model for head models comprising up to five layers. This is also true for the complete, six-layer phantom in the the h-stroke case, while the case of i-stroke and six layers is the only where less artifacts are observed with the exact initial guess model (Fig 7).

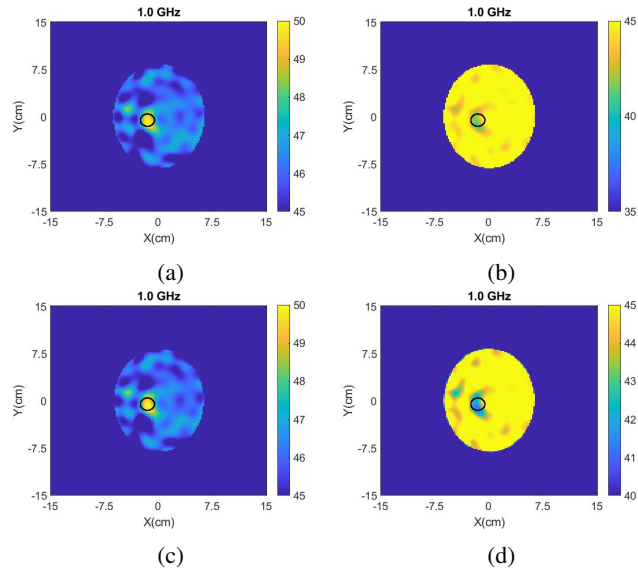


Fig. 3: Reconstructed dielectric constant of our head model including the skin and average brain layers, for the cases of hemorrhagic (left) and ischemic stroke (right). Top: Homogeneous forward model; Bottom: Forward model that includes the skin and average brain layers.

Fig. 8 plots the reconstruction errors of  $\epsilon_\infty$  in the target area, as a function of DBIM iteration number. In most cases,

the error values are similar for the homogeneous and multi-layer models, for both hemorrhagic and ischemic stroke. As also noted for the images, the six-layer model is the only case where the error for the i-stroke (but not for the h-stroke) is higher for the homogeneous initial guess model. These results are in agreement with our observations from the reconstructed images.

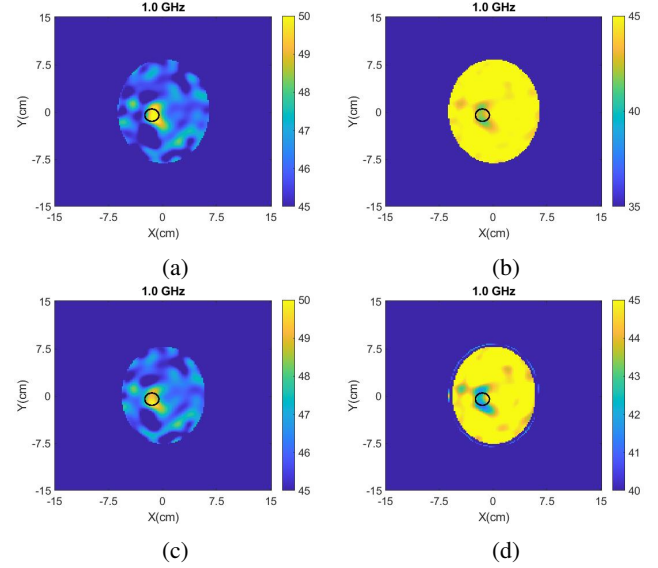


Fig. 4: Reconstructed dielectric constant of our head model including the skin, fat and average brain layers, for the cases of hemorrhagic (left) and ischemic stroke (right). Top: Homogeneous forward model; Bottom: Forward model that includes the skin, fat and average brain layers.

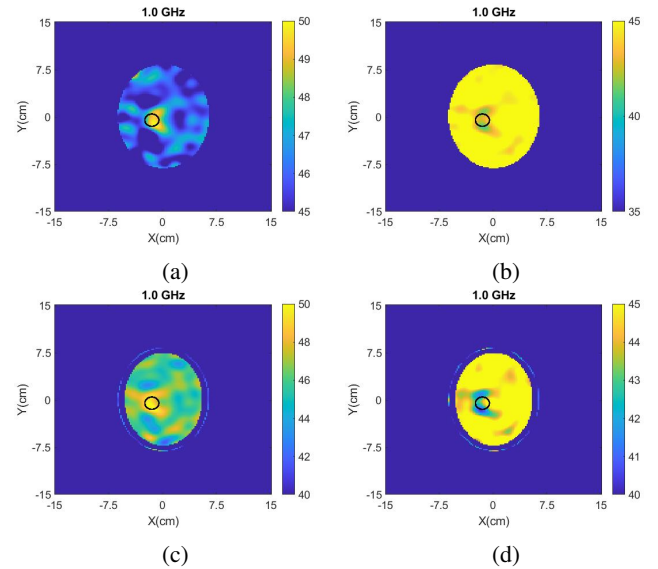


Fig. 5: Reconstructed dielectric constant of our head model including the skin, fat, bone and average brain layers, for the cases of hemorrhagic (left) and ischemic stroke (right). Top: Homogeneous forward model; Bottom: Forward model that includes the skin, fat, bone and average brain layers.

### IV. CONCLUSION

We have investigated how stroke detection and differentiation can be impacted by knowing only approximately the

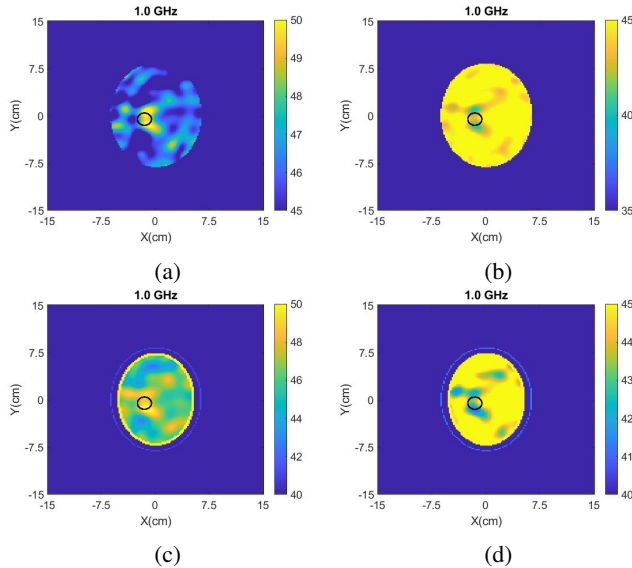


Fig. 6: Reconstructed dielectric constant of our head model including the skin, fat, bone, CSF and average brain layers, for the cases of hemorrhagic (left) and ischemic stroke (right). Top: Homogeneous forward model; Bottom: Forward model that includes the skin, fat, bone, CSF and average brain layers.

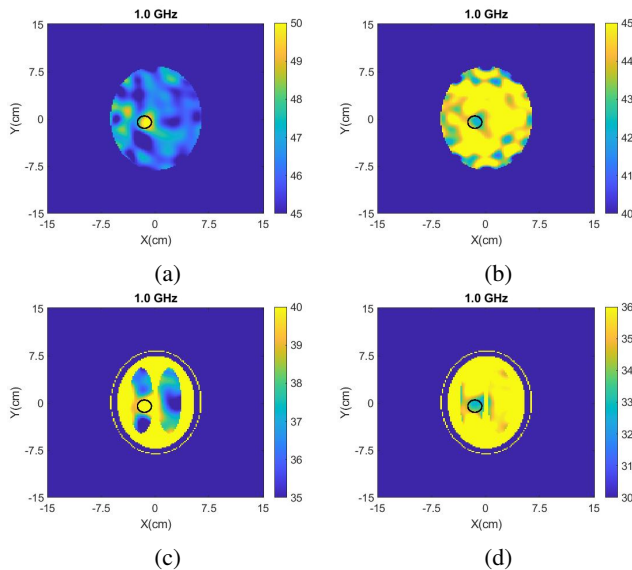


Fig. 7: Reconstructed dielectric constant of our head model including all six layers, for the cases of hemorrhagic (left) and ischemic stroke (right). Top: Homogeneous forward model; Bottom: Forward model that includes all the head layers.

head tissue distribution, using a multi-layered phantom and the DBIM-TwIST algorithm. To this end, we studied two different initial guess scenarios: one of a homogeneous head phantom, and one of an exact head phantom of increasing complexity. The use of these scenarios as the “no-target” case leads to different calibration data, which is then applied to our imaging algorithm.

Our results indicate that the use of a homogeneous model for calibrating and initializing our imaging algorithm produces slightly better reconstructions than using an exact multi-layer model. This is counter-intuitive, but it may be attributed to the fact that there is a mismatch in the dielectric

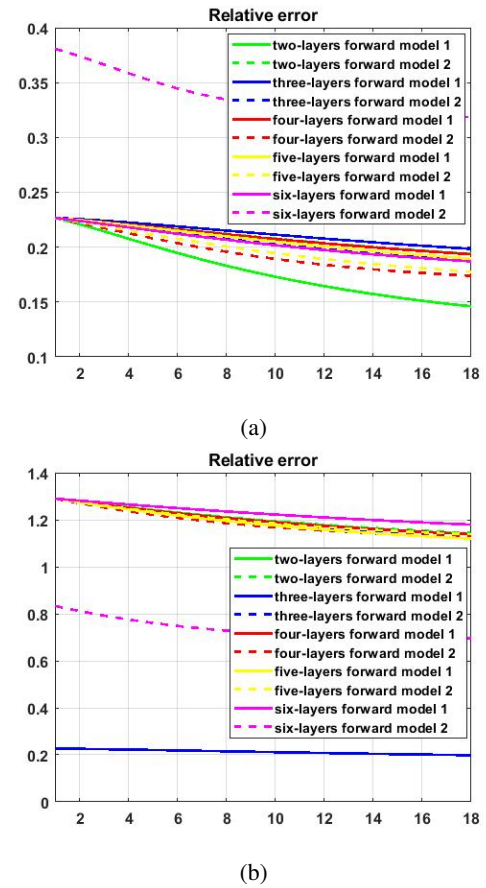


Fig. 8: Reconstruction errors of  $\epsilon_{\infty}$  in (3) inside the target area at 1.0 GHz for (a) h-stroke, and (b) i-stroke, and the different “initial guess” models shown in the legends.

values between the CST multi-layer model and the Debye models used by our FDTD solver. A similar, or possibly worse, mismatch would occur with experimental data. The case of ischemic stroke and the full, six-layer phantom is the only one where we achieve better results with the exact initial guess model.

These results suggest that calibrating with a head phantom that models as many brain tissues as possible may not be preferable for detecting stroke, due to possible mismatches between the true and modeled properties of these tissues. We note, however, that this is only a preliminary study that must also be confirmed experimentally, which is one of our future work objectives.

## REFERENCES

- [1] S. S. Virami, A. Alonso, E. J. Benjamin, M. S. Bittencourt, C. W. Callaway, A. P. Carson, A. M. Chamberlain, A. R. Chang, S. Cheng, F. N. Delling, et al., “Heart disease and stroke statistics—2020 update: a report from the american heart association,” *Circulation*, vol. 141, 9, pp. e139–e596, 2020.
- [2] A. Tobon Vasquez, R. Scapaticci, G. Turvani, G. Bellizzi, D. O. Rodriguez-Duarte, N. Joachimowicz, B. Duchêne, E. Tedeschi, M. R. Casu, L. Crocco, et al., “A prototype microwave system for 3d brain stroke imaging,” *Sensors*, vol. 20, 9, pp. 2607, 2020.
- [3] R. Chandra, H. Zhou, I. Balasingham, and R. M. Narayanan, “On the opportunities and challenges in microwave medical sensing and imaging,” *IEEE transactions on biomedical engineering*, vol. 62, 7, pp. 1667–1682, 2015.
- [4] L. Crocco, I. Karanasiou, M. L. James, R. C. Conceição, and Raquel Cruz, *Emerging Electromagnetic Technologies for Brain Diseases Diagnostics, Monitoring and Therapy*, Springer, 2018.

- [5] M. Azghani, P. Kosmas, and F. Marvasti, "Microwave medical imaging based on sparsity and an iterative method with adaptive thresholding," *IEEE transactions on medical imaging*, vol. 34, 2, pp. 357–365, 2014.
- [6] F. Gao, B. D. Van Veen and S. C. Hagness, "Sensitivity of the Distorted Born Iterative Method to the initial guess in microwave breast imaging," in *IEEE Transactions on Antennas and Propagation*, vol. 63, no. 8, pp. 3540–3547, Aug. 2015.
- [7] V. Zhurbenko, "Challenges in the design of microwave imaging systems for breast cancer detection," *Advances in Electrical and Computer Engineering*, vol. 11, 1, pp. 91–96, 2011.
- [8] G. Zubal, C. R. Harrell, E. O. Smith, Z. Rattner, G. Gindi, and P. B. Hoffer, "Computerized three-dimensional segmented human anatomy," *Medical Physics*, vol. 21, 2, pp. 299–302, 1994.
- [9] O. Karadima, M. Rahman, I. Sotiriou, N. Ghavami, P. Lu, S. Ahsan and P. Kosmas, "Experimental validation of microwave tomography with the DBIM-TwIST algorithm for brain stroke detection and classification," *Sensors*, vol. 20, 3, pp. 840, 2020.
- [10] O. Karadima, M. Rahman, I. Sotiriou, N. Ghavami, P. Lu, S. Ahsan and P. Kosmas, "Experimental validation of microwave tomography with the DBIM-TwIST algorithm for brain stroke detection and classification," *Sensors*, vol. 20, 3, pp. 840, 2020.
- [11] Z. Miao and P. Kosmas, "Multiple-frequency DBIM-TwIST algorithm for microwave breast imaging," *IEEE Transactions on Antennas and Propagation*, vol. 65, 5, pp. 82507–2516, 2017.
- [12] J. D. Shea, P. Kosmas, S.C. Hagness, and B. D. Van Veen, "Three-dimensional microwave imaging of realistic numerical breast phantoms via a multiple-frequency inverse scattering technique," *Medical physics*, vol. 37, 8, pp. 4210–4226, 2010.
- [13] P. Lu and P. Kosmas, "Three-dimensional microwave head imaging with gpu-based fdtd and the dbim method," under preparation.